CMS Physics Analysis Summary

Contact: cms-pag-conveners-susy@cern.ch 2013/07/19

Search for New Physics in the Multijets and Missing Momentum Final State in Proton-Proton Collisions at $\sqrt{s} = 8$ TeV

The CMS Collaboration

Abstract

A search for new physics is reported in multijet events with large missing transverse momentum produced in proton–proton collisions at $\sqrt{s} = 8$ TeV using a data sample corresponding to 19.5 fb^{-1} collected with the CMS detector at the Large Hadron Collider. The data sample is divided into three jet multiplicity regions of 3–5, 6–7, and $\geq$ 8 jets, and studied further in bins of two sensitive variables — the scalar sum of jet transverse momenta and missing transverse momentum. The observed numbers of events are consistent with the standard model expectations which are determined directly from the collision data. Exclusion limits are presented for several simplified supersymmetric model topologies. The squark masses are excluded up to 0.75 TeV in the case where the squarks decay to a jet and the lightest supersymmetric particle. The gluino masses are excluded up to 1.1 TeV when the gluinos decay to two jets and the lightest supersymmetric particle.

1 Introduction

The standard model (SM) of particle physics successfully describes a wide variety of observations in high energy physics experiments. The recent discovery of a new scalar boson with mass of about 126 GeV at the Large Hadron Collider (LHC) [1, 2] seems to mark another success for the SM, as all of the boson's properties measured so far are consistent with the expected characteristics of the long-sought Higgs boson. However, the SM is incomplete and considered only an effective approximation of a more complete theory. For example, it does not have any candidates for dark matter which is postulated to explain astrophysical observations [3], and in addition the Higgs boson mass is unstable against quadratically-divergent quantum loop corrections in the SM. Thus, there are strong reasons to search for phenomena beyond the SM.

In this paper, we present a generic search for new physics beyond the SM in events with multiple jets and large missing transverse momentum, using a data set of an integrated luminosity of 19.5 fb^{-1}, which has been collected in 8 TeV pp collisions at the LHC. This final state is motivated by many extensions of the SM [4–6]. Among these, Supersymmetry (SUSY) is the most explored one and addresses various shortcomings of the SM. SUSY postulates a new symmetry that relates fermionic and bosonic degrees of freedom and introduces a superpartner of each SM particle. These SUSY particles can mitigate the quantum loop corrections due to SM particles and thus stabilize the Higgs boson mass. In *R*-parity-conserving models [7], SUSY particles are produced in pairs, and the lightest SUSY particle (LSP) is stable. If weakly-interacting and neutral, the LSP is a good candidate for dark matter.

At the LHC, both the CMS and ATLAS Collaborations have published SUSY search results in the all-hadronic channel [8–20] which were sensitive to the production of squarks and gluinos (superpartners of quarks and gluons) and their decays to a final state containing jets and stable weakly-interacting particles. In all these searches, the observed numbers of events were consistent with SM background expectations, and exclusion limits were set in the context of the constrained minimal supersymmetric extension of the standard model (CMSSM) [21–23] and various simplified models [24, 25]. Contrary to the CMSSM case, the masses of primary particles and the LSP are free parameters in simplified models and thus allow study of large parts of the parameter space of SUSY and SUSY-like theories. The simplified models of squark-squark production and gluino-gluino production are used to interpret search results in this paper.

This analysis follows previous inclusive searches [9, 12] which required at least three jets in the final state. These searches were most sensitive to the simple decay chains of squarks and gluinos. In order to make the analysis more sensitive to a variety of final state topologies resulting from longer cascades of squarks and gluinos, and hence a large number of jets in the event, the events are sub-divided into three exclusive jet multiplicity regions: N_{jets} =[3–5], [6–7], and [$\geq$8]. This new extension of the search to higher jet multiplicities is motivated by the "natural" SUSY models in which the gluino decays often into top quarks. While other analyses exploit the presence of b jets in signal events to discriminate against background [17, 18], this analysis is following a complementary strategy by requiring a large number of jets, and thus is keeping the signal efficiency for fully hadronic final states as high as possible.

The events are further categorized according to the total visible hadronic activity H_{T} and the momentum imbalance $\not{H}_{\text{T}}$, defined in the direction transverse to the beam.

The main SM processes contributing to this final state are: an irreducible background from Z+jets events, with the Z boson decaying to a pair of neutrinos, denoted as $\text{Z}(\nu\bar{\nu})$+jets; W+jets and $\text{t}\bar{\text{t}}$ events, with a W boson decaying directly or via a τ to an e or μ that is not reconstructed, isolated, or out of acceptance; or to a τ that decays hadronically. In all these cases, one or more

neutrinos provide a source of genuine missing transverse momentum. The third background category is QCD multijet events with large missing transverse momentum from leptonic decays of heavy-flavour hadrons inside the jets, jet energy mismeasurement, or instrumental noise and non-functioning detector components. All these backgrounds are determined from the data, relying on simulation as little as possible.

2 The CMS Detector and Event Reconstruction

The CMS detector is a multi-purpose apparatus, described in detail in Ref. [26]. Charged particle trajectories are measured by the silicon pixel and strip tracker, covering $|\eta| < 2.5$, where the pseudorapidity η is defined as $\eta = -\ln\tan(\theta/2)$, with θ being the polar angle of the trajectory of the particle with respect to the counterclockwise beam direction. Immersed in the 3.8 T magnetic field provided by a superconducting solenoid of 6m in diameter that also encircles the calorimeters, the tracker provides transverse momentum resolution of approximately 1.5% for charged particles with transverse momentum $p_{\mathrm{T}} \sim 100\,\mathrm{GeV}$. A lead-tungstate crystal electromagnetic calorimeter and a brass and scintillator hadronic calorimeter surround the tracking volume and cover the region $|\eta| < 3$. Quartz and steel forward hadron calorimeters extend the coverage to $|\eta| \leq 5$. Muons are identified in gas ionization detectors embedded in the steel return yoke of the magnet. The data pertinent to this analysis are recorded using a two level trigger system described in Ref. [26].

The recorded events are reconstructed using the particle-flow algorithm [27]. This algorithm reconstructs particles in each event, namely charged hadrons, photons, neutral hadrons, muons, and electrons, using the information from the tracker, the calorimeters, and the muon system. All reconstructed particles are clustered into jets using the anti-k_T clustering algorithm with the size parameter $D = 0.5$ [28]. Corrections are applied to account for the variation of the jet response on p_{T} and η [29, 30]. Contributions from additional pp collisions overlapping with the event of interest (pileup pp collisions) are mitigated using the Fastjet tools [31, 32], and by discarding charged particles originating from pileup interaction vertices.

3 Sample Selection

The data sample used for this analysis is collected by triggering on $H_{\mathrm{T}} > 350$ GeV and missing transverse momentum > 100 GeV. The trigger efficiencies are measured to be >99% for an offline $H_{\mathrm{T}} > 500$ GeV and $\not{H}_{\mathrm{T}} > 200$ GeV for all jet multiplicities used in this search.

The search selection starts from a loose baseline selection using the following requirements after the trigger:

- $N_{\mathrm{jets}} \geq 3$, where N_{jets} is the number of jets with $p_{\mathrm{T}} > 50\,\mathrm{GeV}$ and $|\eta| < 2.5$.
- $H_{\mathrm{T}} > 500\,\mathrm{GeV}$, with $H_{\mathrm{T}} = \sum_{\mathrm{jets}} p_{\mathrm{T}}$ where the sum is carried over jets with $p_{\mathrm{T}} > 50\,\mathrm{GeV}$ and $|\eta| < 2.5$.
- $\not{H}_{\mathrm{T}} > 200\,\mathrm{GeV}$, with $\not{H}_{\mathrm{T}} = |\vec{\not{H}}_{\mathrm{T}}| = |-\sum_{\mathrm{jets}} \vec{p}_{\mathrm{T}}|$ where in this case jets are required to satisfy $p_{\mathrm{T}} > 30\,\mathrm{GeV}$ and $|\eta| < 5$.
- $|\Delta\phi(\vec{p}_{\mathrm{T}}^{\,\mathrm{jet1}}, \vec{\not{H}}_{\mathrm{T}})| > 0.5$, $|\Delta\phi(\vec{p}_{\mathrm{T}}^{\,\mathrm{jet2}}, \vec{\not{H}}_{\mathrm{T}})| > 0.5$, and $|\Delta\phi(\vec{p}_{\mathrm{T}}^{\,\mathrm{jet3}}, \vec{\not{H}}_{\mathrm{T}})| > 0.3$ (rad), vetoing events in which $\not{H}_{\mathrm{T}}$ is aligned in the transverse plane along one of the three most energetic jets. This requirement rejects most of the QCD multijet events in which a single mismeasured jet yields a high $\not{H}_{\mathrm{T}}$.

- Events containing isolated muons or electrons with $p_T > 10$ GeV are vetoed in order to reject $t\bar{t}$ and W/Z+jets events with leptons in the final state.
- In addition, events affected by instrumental effects, particles from non-collision sources, or poorly reconstructed kinematic variables are rejected (event cleaning) [33]. Events are also rejected if a jet with $p_T > 30$ GeV has a photon p_T fraction larger than 0.95 or a neutral hadron p_T fraction larger than 0.90.

To increase the sensitivity of the search for generic final states containing jets and $\not{H}_T$, a sample of 11753 events selected in the baseline region is divided according to jet multiplicity into three exclusive regions with N_{jets} =[3–5], [6–7] and [$\geq$8]. For each jet multiplicity selection, the events are further divided into subsamples defined in terms of H_T and $\not{H}_T$ to enhance the sensitivity of the search in different kinematic regions. The 36 search regions used in this analysis are listed in the first column of Table 1.

Several Monte Carlo (MC) simulation samples are used to model the signal as well as to develop and validate the background estimations. The $t\bar{t}$, W/Z+jets, γ+jets, and QCD multijet background samples are produced using the MADGRAPH5 [34] generator, interfaced with the PYTHIA 6.4.24 [35] parton-shower model, and scaled up to the next-to-leading order (NLO) or next-to-next-to-leading order (NNLO) cross section predictions [36, 37]. The SUSY signal production is simulated with PYTHIA 6.4.24, the CTEQ6L [38] parton distribution functions (PDFs), and a CMS custom underlying event tuning [39]. The generated events are passed through a GEANT4-based [40] detector simulation and are reweighted to match the distribution of pileup pp interactions as observed in the data.

4 Data-Driven Background Estimation

The SM backgrounds mainly consist of $Z(\nu\bar{\nu})$+jets events and $W(\ell\nu)$+jets events from W or $t\bar{t}$ production (ℓ = e, μ, or τ) and of QCD multijet events. The relative contribution of these backgrounds varies in different search regions. In this search, all the backgrounds are measured from data using methods similar to those used in [9, 12]. The $W(\ell\nu)$+jets events pass the search selection when the e/μ escapes detection (lost-lepton background) or a τ decays hadronically (hadronic-τ background). The lost-lepton background is estimated by reweighting events in a μ+jets event sample from data with measured lepton (in)efficiencies. The estimation of the hadronic-τ background starts from a similar μ+jets sample where the muon is replaced by a hadronic-τ jet using a p_T response template obtained from the CMS simulation. The irreducible $Z(\nu\bar{\nu})$+jets background events are estimated using $\gamma+$ jets events exploiting their electroweak correspondence to the Z production at high boson p_T. The QCD multijet events also contribute to the background when leptonic decays of heavy-flavor hadrons inside jets or jet energy mismeasurements lead to a large $\not{H}_T$. This background is measured using a "Rebalance and Smear" (R+S) method. It predicts QCD multijet kinematics by applying measured jet resolution functions to smear seed events that are obtained by a procedure that produces well-balanced events from inclusive multijet data. The contributions from other SM processes are found to be negligible. The methods to estimate these backgrounds using data events are summarized below.

4.1 Estimation of $Z(\nu\bar{\nu})$+jets Background

The contribution of $Z(\nu\bar{\nu})$+jets events to the search regions is estimated using γ+jets events in the collision data. The Z boson and photon exhibit similar kinematic properties at high p_T and the hadronic component of events is similar in the two cases [41–44]. To mimic the missing momentum due to the neutrinos, the photon candidate is removed from the event, and H_T and

$\not{H}_T$ are recalculated. The $Z(\nu\bar{\nu})$+jets events are predicted by weighting the γ+jets events for the reconstruction efficiency and kinematic acceptance of photons, and the difference in production cross section of the two processes.

The γ+jets events used in this analysis are collected by triggering on events with a γ candidate and H_T online. The trigger requirements are measured to be fully efficient for the baseline selection. The offline photon candidates are required to be isolated in the tracker and calorimeters and to have their shower shape consistent with prompt photons. The residual QCD contribution to the γ+jets control sample is measured using a template method where a variable which characterizes the lateral shape of photon showers ($\sigma_{i\eta i\eta}$) is fitted with the sum of the expected background and signal shapes. The signal template is taken from simulation whereas the background is obtained from a data sideband region. The photon candidates in the sideband must pass a very loose photon identification and isolation and also fail one of the stringent photon isolation requirements. On average, 93% of selected candidate γ+jet events are found to arise from photon+jet production.

The sample of photon events is then scaled by a phenomenological ratio relating γ+jets and $Z(\nu\bar{\nu})$+jets cross sections and the photon reconstruction efficiency and acceptance. The phenomenological Z/γ ratio is studied in detail as a function of H_T, $\not{H}_T$, and N_{jets}, using events simulated with MADGRAPH (up to 4 partons) and run through PYTHIA parton showering for additional jets. The ratio increases with $\not{H}_T$ before flattening out (Fig. 1(b)) whereas the ratio changes by only (12 $\pm$ 5)% from H_T = 500 GeV to H_T = 1500 GeV, the region of interest to this search. It is parametrized as a linear function of N_{jets} in several $\not{H}_T$ ranges (200 $< \not{H}_T <$ 300 GeV, 300 $< \not{H}_T <$ 450 GeV, and $\not{H}_T >$ 450 GeV) as shown in Fig. 1(c).

In the earlier searches [9, 12] which used events with $N_{jets} \geq 3$ inclusively, a theoretical uncertainty on the phenomenlogical ratio is assigned by comparing the value of Z/γ from a leading order event generator program to that from a full NLO calculation as described in [44]. For the present search, $Z \to \mu^+\mu^-$+jets and γ+jets events in data are used to constrain the theoretical uncertainty on the Z/γ ratio. The $Z \to \mu^+\mu^-$+jets events have been selected by requiring two opposite sign muons passing the muon definition of the lepton veto and forming an invariant mass within an interval of 20 GeV around the Z boson mass. The ratio of $Z \to \mu^+\mu^-$+jets and γ+jets events in the data to that in the MC simulation is parametrized as a function of N_{jets} using a linear function as shown in Fig. 1 (d). This parametrization is used to correct the Z/γ measured in the MC simulation for a given jet multiplicy and the statistical uncertainty on the fit is assigned as an uncertainty. This procedure results in an uncertainty of 17–18%, 19–21% , and 22–24% for the search regions of N_{jets} = [3–5], [6–7] and [$\geq$8] selections respectively. The modeling of photon identification and isolation in MC leads to 2-5%, 10-20%, and 20-25% in the aforementioned N_{jets} bins. The subtraction of events with non-prompt photons from QCD multijet events amounts to less than a 5% uncertainty on the final prediction of $Z(\nu\bar{\nu})$+jets events.

4.2 Estimation of lost-lepton background

The $W(\ell\nu)$+jets events (ℓ = e or μ) from W or top quark production constitute a background when an electron or muon is not identified or isolated, or is out of the detector acceptance, and therefore passes the lepton veto described in Section 3. Events with lost electrons or muons from leptonically decaying taus are also taken into account. This background is estimated from a μ+jets control sample, selected with the same criteria as those used for the search except that we require an event to have exactly one well reconstructed and isolated μ with $p_T^\mu >$10 GeV. The transverse mass $m_T = \sqrt{2p_T^\mu \not{E}_T[1-\cos(\Delta\phi)]}$ is required to be less than 100 GeV

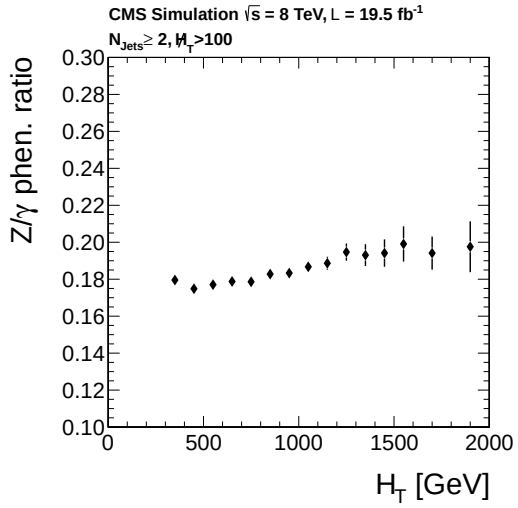

(a) Z/γ ratio vs. H_{T}

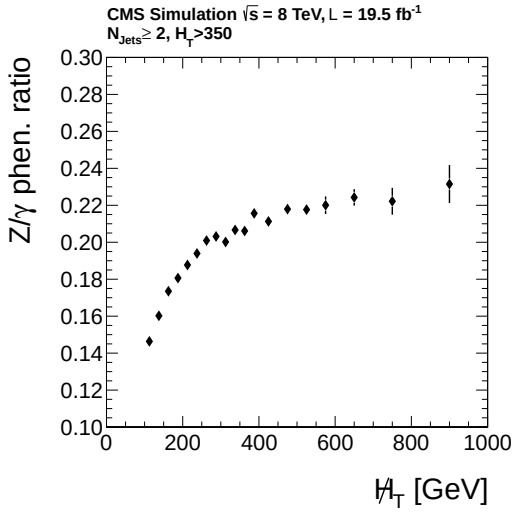

(b) Z/γ ratio vs. $\not{H}_{\mathrm{T}}$

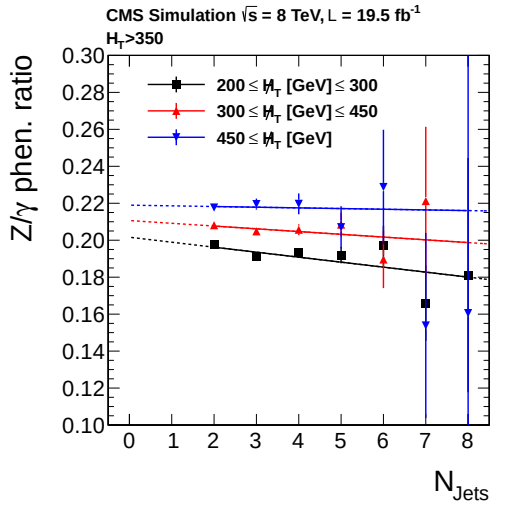

(c) Z/γ ratio vs. N_{Jets}

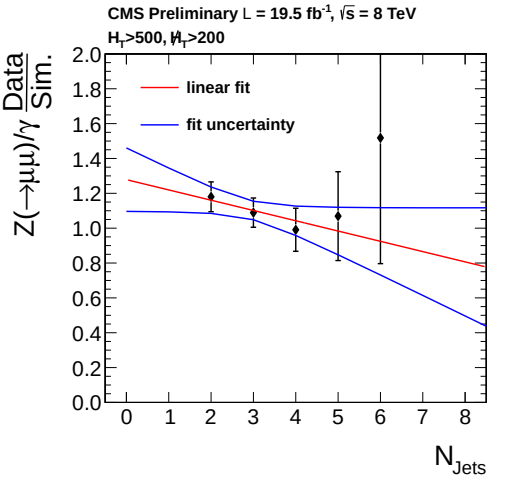

(d) $Z(\mu\mu)/\gamma$ double ratio (data/MC) vs. N_{Jets}

Figure 1: Z/γ ratio vs. H_{T} ((a)), $\not{H}_{\mathrm{T}}$ ((b)), and N_{jets} ((c) in the 3 $\not{H}_{\mathrm{T}}$ bins fitted by a linear function). Figure (d) shows Z/γ double ratio (data/simulation) with $Z \to \mu^{+}\mu^{-}$+jets events; the linear fit and its variance band is overlaid.

in order to select events containing a $W \to \mu\nu$ decay and to suppress possible new physics signal contamination, i.e., the signal events resulting in the μ+jets sample being used for the background estimation. Here $\not\!\!E_T$ is the missing transverse energy [33], and $\Delta\phi$ is the azimuthal angle between the $\vec{p_T}^{\mu}$ and the $\vec{\not\!\!E}_T$ directions.

Using the reconstruction and isolation efficiencies $\epsilon^{e,\mu}_{reco}$ and $\epsilon^{e,\mu}_{iso}$ of the electrons and muons, the events in the isolated muon control sample are weighted according to

- $(1/\epsilon^{\mu}_{iso})\,[(1-\epsilon^{e,\mu}_{reco})/\epsilon^{\mu}_{reco}]$ to predict events with unidentified leptons, and
- $(\epsilon^{e,\mu}_{reco}/\epsilon^{\mu}_{reco})\,[(1-\epsilon^{e,\mu}_{iso})/\epsilon^{\mu}_{iso}]$ to estimate events with nonisolated leptons in the signal region.

The lepton isolation and reconstruction efficiencies, and kinematic acceptance are obtained from MC simulation of W+jets and $t\bar{t}$ events and are determined in bins of N_{jets}, H_T, and $\not\!\!H_T$ following closely the search bin definition.

This estimation method based on the collision data is validated by predicting the lost lepton background using a single muon sample from simulated $t\bar{t}$ and W + jets events, and comparing the predicted and the expected true detector-level distributions. A comparison of the predicted and the expected distributions of H_T, $\not\!\!H_T$, and N_{jets} for events with a lost-lepton in the baseline selection region are shown in Fig. 2. The predicted distributions closely reproduce the expected distribution of sensitive variables used for this search.

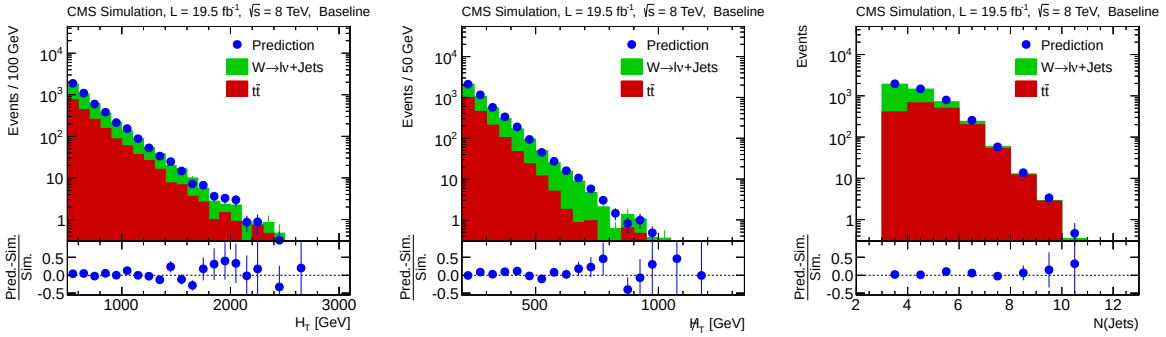

Figure 2: Predicted distributions of H_T (left), $\not\!\!H_T$ (middle) and N_{jets} (right) compared to those expected in the $t\bar{t}$ and W + jets MC simulated events containing an undetected lepton (e or μ).

The prediction is obtained by applying this method to the μ+jets sample collected using the same $H_T + \not\!\!E_T$ trigger which is used to collect the signal events. The predicted lost-lepton events and uncertainties for each search region are listed in Table 1. The dominant uncertainties on the lost-lepton prediction arise from the limited statistics of the muon sample selected from data for most of the search regions. In order to account for a possible difference in lepton reconstruction and isolation efficiencies in data and MC, these are estimated by applying a "tag and probe" method [45] on $Z \to \mu^+\mu^-$ events in data and simulation. The lepton reconstruction and isolation efficiencies are measured in bins of lepton p_T and $\Delta R = \sqrt{(\Delta\eta)^2 + (\Delta\phi)^2}$ relative to the closest jet to make these insensitive to the kinematic differences between $Z(\ell^+\ell^-)$+jets events and the $t\bar{t}$ and W+jets events. Relative differences between the predictions using efficiencies extracted from data and MC results in 10–25%, 10–30% and 15–24% for the search bins in N_{jets} =[3–5], [6–7] and [$\geq$8] respectively. An additional uncertainty of 15% for N_{jets} =[3–5] and 40% for N_{jets} =[$\geq$6] is assigned based on the statistical precision of the validation of this background estimation method. The variations of the parton density functions following the recommendation of Ref. [46] change the muon acceptance, and leads to less than 4% uncer-

tainty on the final prediction. An additional uncertainty of 3% is assigned to account for a possible difference in data and MC on the acceptance of m_{T} selection and is mostly expected to arise from $\not\!\!E_{\mathrm{T}}$ outliers.

4.3 Hadronic τ background estimation

The hadronic decay of τ leptons (τ_{h}) is the second important component of the background due to W + jets or $\mathrm{t\bar{t}}$ events in the search regions. The presence of neutrinos in the final state results in $\not\!\!H_{\mathrm{T}}$, and the event passes the lepton veto because the hadronically decaying τ is reconstructed as a jet. This background is estimated from a sample of μ+jets events, selected from inclusive single μ or $\mu + \geq$2-jet triggers by requiring exactly one μ with $p_{\mathrm{T}}^{\mu} > 20\,\mathrm{GeV}$ and $|\eta| < 2.1$. As in the estimation of the lost-lepton background, only the events with $m_{\mathrm{T}} < 100$ GeV are considered. The μ+jets and τ_{h} +jets events arise from the same physics processes, hence the hadronic component of the two samples is the same except for the response of the detector to a muon or a τ_{h} jet. To account for this difference, the muon is replaced by a τ_{h} jet with the p_{T} taken randomly from a simulated response function for a hadronically-decaying τ lepton. The N_{jets}, H_{T}, and $\not\!\!H_{\mathrm{T}}$ of the event are recalculated including this τ_{h} jet, and the search selections are applied to predict the τ_{h} background. The τ_{h}-jet response function $p_{\mathrm{T}}^{\mathrm{jet}}/p_{\mathrm{T}}^{\tau}$ is obtained from simulated $\mathrm{t\bar{t}}$ and $\mathrm{W}(\tau\nu)$+jets events by matching the reconstructed τ jet with the generated τ lepton decaying hadronically, in the bins of the originating τ momentum. In order to sample the complete response template this procedure is repeated multiple times for each event. Corrections are applied to account for the trigger efficiency, acceptance, and efficiency of the μ selection, and the ratio of branching fractions $\mathcal{B}(\mathrm{W} \to \tau_{\mathrm{h}}\nu)/\mathcal{B}(\mathrm{W} \to \mu\nu) = 0.6476 \pm 0.0024$ [47]. The predicted τ_{h} background and uncertainties are shown in Table 1 for all the search regions.

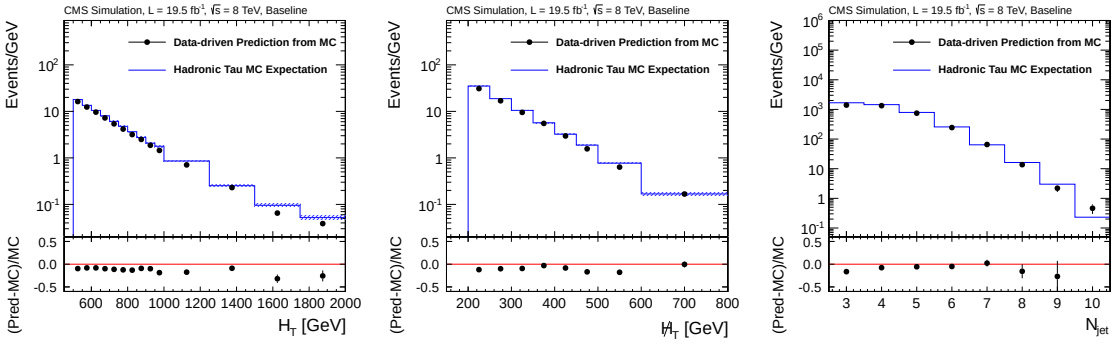

Figure 3: Comparison of predicted distributions of H_{T} (left), $\not\!\!H_{\mathrm{T}}$ (middle) and N_{jets} (right) with the expectation in MC simulated $\mathrm{t\bar{t}}$ and W + jets events containing a hadronically decaying τ lepton. Only the statistical uncertainties are shown on the predicted distributions.

The τ_{h} background estimation method is validated by applying it to the W and $\mathrm{t\bar{t}}$ MC samples. A comparison of predicted distributions of H_{T}, $\not\!\!H_{\mathrm{T}}$, and N_{jets} with true detector-level τ_{h} background events is shown in Fig. 3 for the baseline selection. To evaluate the performance of the method in events with varying hadronic activity, the method is validated in each search bin. For each of the three jet multiplicity regions used in the analysis the prediction is corrected for the average bias observed for a given jet multiplicity. Uncertainties of 8.9%, 15.1% and 21.3% are assigned to the predicted rate in various H_{T} and $\not\!\!H_{\mathrm{T}}$ search regions for events with N_{jets} =[3–5], [6–7] and [$\geq$8] respectively, mainly to reflect the statistical power of this validation. Due to the multiple sampling of the response template, the statistical uncertainty on the prediction is

evaluated with a set of pseudo-experiments using a bootstrap technique [48]. The other main systematic uncertainties in the hadronic-τ background estimation arise from the μ acceptance (3–22%) and the τ-jet response function (1–15%). An additional uncertainty of 1–8% is assigned on the predicted events to account for possible differences in data and MC on the acceptance of the m_{T} selection.

4.4 Estimation of QCD Multijet Background

The QCD multijet events contribute to the search regions when leptonic decays of heavy-flavor hadrons inside jets accompanied by neutrinos or jet energy mismeasurements lead to a large $\not{H}_{\mathrm{T}}$. A majority of these events are rejected by requiring $\not{H}_{\mathrm{T}}$ >200 GeV and by vetoing the events in which $\vec{\not{H}}_{\mathrm{T}}$ is aligned to any one of the leading three jets as described in Section 3. The remaining events are estimated from collider data recorded with a set of triggers having an H_{T} threshold ranging from 350 to 750 GeV, using a "Rebalance and Smear" method [9].

In the rebalance step, the momenta of the jets with p_{T} >10 GeV in these events are adjusted within the jet p_{T} resolution, using a kinematic fit such that the events are balanced in the transverse plane. Each rebalanced event is used multiple times to estimate the QCD multijet background in the search regions. The data samples used include the electroweak contributions not removed by the lepton veto and any potential new physics events; however, their cross-section is negligible compared to the QCD multijet cross section. The rebalanced event sample is a good estimator of QCD multijet events at the level of particle jets. Using a p_{T} threshold on the jets results in an additional measured imbalance in the event. Thus the rebalancing procedure assigns a p_{T} to a jet which is larger than its true p_{T}. To account for this, the observed jet momenta are scaled by a factor before re-balancing. This scaling factor is determined from simulation by comparing the rebalanced jets with the true particle jets. The correction factors are determined in QCD multijet events produced using two different event generators PYTHIA and MADGRAPH, and events with different average pileup are found to be similar.

The jet p_{T} values in the rebalanced events are then smeared with the measured jet resolutions to predict the QCD multijet background. The jet p_{T} response functions are determined as a function of p_{T} and η using high-statistics multijet MC MADGRAPH samples that include heavy flavor quarks. The width and tail of the p_{T} response functions are subsequently adjusted to account for the differences in the resolutions measured in the simulated and the collider data [29]. The width (σ) of the gaussian part of the simulated response is 5 (30)% narrower than what is observed in the data for $|\eta| < 0.5$ ($2.3 < |\eta| < 5.0$). The fraction of jets with response $> 2.5\sigma$ away from the mean value is consistent with the data within statistics.

The main uncertainties in this QCD estimation method arise from the shape of the jet response functions including the Gaussian width, the tails, the heavy flavor contribution, and the effect of pileup pp interactions on jets in an event. The method has been validated in simulated QCD multijet events. A comparison of predicted and true detector level distributions of H_{T}, $\not{H}_{\mathrm{T}}$ and N_{jets} are shown in Fig. 4. A systematic uncertainty ranging from 11 to 86% is assigned to account for the potential residual non-closure of the method masked by the large statistical uncertainties of the simulated QCD sample. As the uncertainty on the simulated QCD background is very large in some of the search regions, the non-closure uncertainty is obtained from QCD enriched sidebands, i.e. for $100 < \not{H}_{\mathrm{T}} < 200$ GeV or an inverted $|\Delta\phi(\vec{p}_{\mathrm{T}}^{\,\mathrm{jet1,2,3}}, \vec{\not{H}}_{\mathrm{T}})|$ cut. If statistically significant, the larger deviation is taken as a systematic uncertainty on the prediction. Because of limited amount of events in individual search bins, this uncertainty is evaluated for each jet multiplicity bin for H_{T} smaller and larger than 1000 GeV, inclusive in $\not{H}_{\mathrm{T}}$. The predicted QCD multijet background contributions to the search bins are given in Table 1.

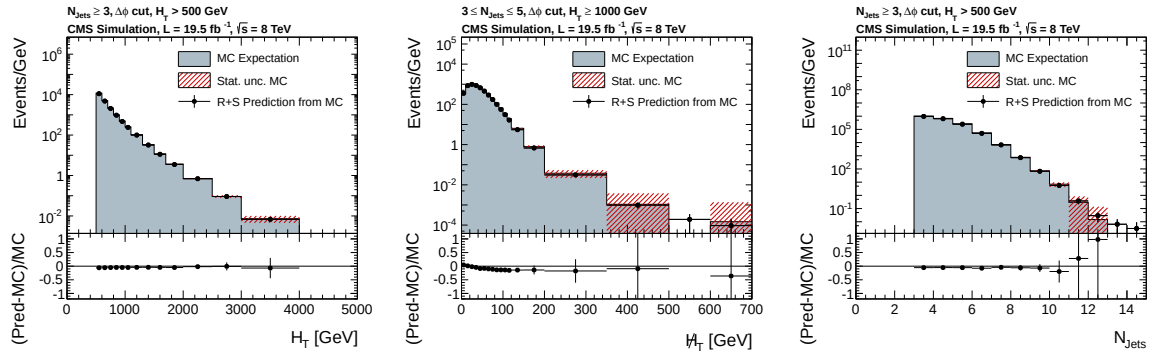

Figure 4: Comparison of QCD multijet prediction to the expectation from a Monte Carlo sample. Only statistical uncertainties are shown as a hashed band around the expectation and an error bar on the prediction. The shown variables are H_T without $\not{H}_T$ selection (left) and $\not{H}_T$ for a high H_T selection (middle) on top and number of jets for the baseline selection (right).

5 Results and Interpretation

The predicted SM background event yields and the number of events observed in data are summarized in Table 1 and Figure 5 for the 36 search regions defined in N_{jets}, H_T, and $\not{H}_T$. The data are consistent with the expected contributions from the SM processes.

The results are interpreted in the context of simplified models (SMS) [24, 25] of new particles which decay directly or via intermediate particles to quarks and a stable undetectable particle. In the context of SUSY, the new particles are either squarks ($\tilde{q}$) or gluinos ($\tilde{g}$) which are assumed to be produced in pairs, and they decay to jets and a neutral weakly interacting particle denoted by $\tilde{\chi}^0$, the lightest supersymmetric particle. The model used here includes the production of $\tilde{g}\tilde{g}$ and $\tilde{q}\tilde{q}$ pairs and their decays for a wide range of $\left(m(\tilde{g}), m(\tilde{\chi}^0)\right)$ and $\left(m(\tilde{q}), m(\tilde{\chi}^0)\right)$ values. The other SUSY particles are assumed to be decoupled. The signal events are generated at leading order using PYTHIA 6.4.24 [35]. The cross sections are determined at the next-to-leading order in the strong coupling constant and include the resummation of soft gluon emission at the accuracy of next-to-leading-log level [49–54]. The distribution of pileup pp interactions matches that observed in the data. The decay modes of squarks and gluinos considered here are $\tilde{q} \to q\tilde{\chi}^0$ and $\tilde{g} \to q\bar{q}\,\tilde{\chi}^0$ respectively, where the branching fraction is assumed to be 100%.

The 95% confidence level (CL) upper limits on the SMS signal cross section are set using the profile likelihood as a test statistic [55–57]. The results from the 36 exclusive search regions are combined into one test-statistic considering the bin-to-bin correlations of the systematic uncertainties. The uncertainties on the background predictions as given in Table 1, the luminosity determination (4.4%), the signal acceptance and efficiency arising from the jet energy scale ($\sim$ 8%), jet energy resolution ($\sim$ 2%), parton distribution functions (PDF) of the proton ($\sim$ 8%), modeling of initial or final state radiation (20%), trigger inefficiency (2%), and the event cleaning procedure (3%) are taken into account when the limits are determined.

The observed and expected 95% CL upper limits on the signal cross section are shown for the production of $\tilde{q}\tilde{q}$ pair with $\tilde{q} \to q + \tilde{\chi}^0$ in Fig. 6a, and $\tilde{g}\tilde{g}$ pair with $\tilde{g} \to q\bar{q} + \tilde{\chi}^0$ in Fig. 6b; in the $m_{\tilde{q}}$-$m_{\tilde{\chi}^0}$ and $m_{\tilde{g}}$-$m_{\tilde{\chi}^0}$ planes. For these models, contours are shown where the signal cross sections from NLO+NLL calculations are excluded. The exclusion contours are also presented when the signal cross section is varied by changing the renormalization and factorization scales by a factor of two and using the PDF uncertainty based on the CTEQ6.6 [58] and MSTW2008 [59] PDF sets. These SMS cross section upper limits may be translated to limits on

Table 1: Predicted event yields for the different background components for the search regions defined in H_T, $\not{H}_T$ and N_{jets} using the 19.5 fb^{-1} dataset. The uncertainties on various backgrounds are added in quadrature to get the uncertainty on total background estimation.

Selection			$Z \to \nu\bar{\nu}$	$t\bar{t}$/W	$t\bar{t}$/W	QCD	Total	Obs.
N_{jets}	H_T	$\not{H}_T$	from γ+jets	$\to e, \mu$+X	$\to \tau_h$+X		background	data
3-5	500-800	200-300	1821.3±326.5	2210.7±447.8	1683.7±171.4	307.4±219.4	6023.1±620.2	6159
3-5	500-800	300-450	993.6±177.9	660.1±133.3	591.9± 62.5	34.5± 23.8	2280.0±232.1	2305
3-5	500-800	450-600	273.2± 51.1	77.3± 17.9	67.6± 9.5	1.3± 1.5	419.5± 55.0	454
3-5	500-800	> 600	42.0± 8.7	9.5± 4.0	6.0± 1.9	0.1± 0.3	57.6± 9.7	62
3-5	800-1000	200-300	215.8± 40.0	277.5± 62.4	191.6± 23.2	91.7± 65.5	776.7±101.6	808
3-5	800-1000	300-450	124.1± 23.7	112.8± 26.9	83.3± 11.2	9.9± 7.4	330.1± 38.3	305
3-5	800-1000	450-600	46.9± 9.8	36.1± 9.9	23.6± 3.9	0.8± 1.3	107.5± 14.5	124
3-5	800-1000	> 600	35.3± 7.5	9.0± 3.7	11.4± 3.2	0.1± 0.4	55.8± 9.0	52
3-5	1000-1250	200-300	76.3± 14.8	103.5± 25.9	66.8± 10.0	59.0± 24.7	305.6± 40.1	335
3-5	1000-1250	300-450	39.3± 8.2	52.4± 13.6	35.7± 6.2	5.1± 2.7	132.6± 17.3	129
3-5	1000-1250	450-600	18.1± 4.4	6.9± 3.2	6.6± 2.1	0.5± 0.7	32.1± 5.9	34
3-5	1000-1250	> 600	17.8± 4.3	2.4± 1.8	2.5± 1.0	0.1± 0.3	22.8± 4.7	32
3-5	1250-1500	200-300	25.3± 5.5	31.0± 9.5	22.2± 3.9	31.2± 13.1	109.7± 17.5	98
3-5	1250-1500	300-450	16.7± 4.0	10.1± 4.4	11.1± 3.6	2.3± 1.6	40.2± 7.1	38
3-5	1250-1500	> 450	12.3± 3.2	2.3± 1.7	2.8± 1.5	0.2± 0.5	17.6± 4.0	23
3-5	>1500	200-300	10.5± 2.8	16.7± 6.2	15.2± 3.4	35.1± 14.1	77.6± 16.1	94
3-5	>1500	> 300	10.9± 2.9	9.7± 4.3	6.5± 2.0	2.4± 2.0	29.6± 5.8	39
6-7	500-800	200-300	22.7± 6.1	132.5± 58.6	127.1± 21.5	18.2± 9.2	300.5± 63.4	266
6-7	500-800	300-450	9.9± 3.1	22.0± 10.8	18.6± 4.3	1.9± 1.7	52.3± 12.1	62
6-7	500-800	> 450	0.7± 0.6	0.0± 1.6	0.1± 0.3	0.0± 0.1	0.8± 1.7	9
6-7	800-1000	200-300	9.1± 2.8	55.8± 25.4	44.6± 8.2	13.1± 6.6	122.6± 27.7	111
6-7	800-1000	300-450	4.2± 1.6	10.4± 5.5	12.8± 3.1	1.9± 1.4	29.3± 6.6	35
6-7	800-1000	> 450	1.8± 1.0	2.9± 2.5	1.3± 0.5	0.1± 0.4	6.1± 2.7	4
6-7	1000-1250	200-300	4.4± 1.6	24.1± 12.0	24.0± 5.5	11.9± 6.0	64.4± 14.6	67
6-7	1000-1250	300-450	3.5± 1.4	8.0± 4.7	9.6± 2.5	1.5± 1.5	22.6± 5.7	20
6-7	1000-1250	> 450	1.4± 0.8	0.0± 1.8	0.8± 0.5	0.1± 0.3	2.3± 2.1	4
6-7	1250-1500	200-300	3.3± 1.3	11.5± 6.5	6.1± 2.5	6.8± 3.9	27.7± 8.1	24
6-7	1250-1500	300-450	1.4± 0.8	3.5± 2.6	2.9± 1.5	0.9± 1.3	8.8± 3.4	5
6-7	1250-1500	> 450	0.4± 0.4	0.0± 1.2	0.1± 0.2	0.1± 0.3	0.5± 1.3	2
6-7	>1500	200-300	1.3± 0.8	10.0± 6.9	2.3± 1.3	7.8± 4.0	21.5± 8.1	18
6-7	>1500	> 300	1.1± 0.7	3.2± 2.8	2.9± 1.2	0.8± 1.1	8.0± 3.3	3
≥8	500-800	> 200	0.0± 0.6	1.9± 1.5	2.8± 1.3	0.1± 0.4	4.8± 2.1	8
≥8	800-1000	> 200	0.6± 0.5	4.8± 2.9	2.7± 1.1	0.5± 0.9	8.7± 3.3	9
≥8	1000-1250	> 200	0.6± 0.5	1.4± 1.5	3.1± 1.2	0.7± 0.9	5.8± 2.2	8
≥8	1250-1500	> 200	0.0± 0.7	5.1± 3.5	1.3± 0.8	0.5± 0.9	6.9± 3.7	5
≥8	1500-	> 200	0.0± 0.6	0.0± 2.1	1.5± 1.0	0.9± 1.3	2.4± 2.8	2

SUSY particle production within more complex models. In the model considered here, $m_{\tilde{g}}$ values below 1.1 TeV for decays via light quarks are excluded. For direct $\tilde{q}\tilde{q}$ production of the first two generations of squarks ($\tilde{u}_{L/R}, \tilde{d}_{L/R}, \tilde{c}_{L/R}, \tilde{s}_{L/R}$) values of $m_{\tilde{q}}$ below 0.75 TeV are excluded for $m_{\tilde{\chi}^0} < 200$ GeV. If only one light squark is light enough to be accessible, $m_{\tilde{q}}$ values below 420 GeV are excluded for $m_{\tilde{\chi}^0} < 100$ GeV.

6 Conclusions

In summary, an inclusive search for supersymmetry has been performed in the multijets and $\not{H}_T$ final state with N_{jets} =[3–5], [6–7], and [≥8], using a data sample corresponding to an integrated luminosity of 19.5 fb^{-1} collected in 8 TeV pp collisions during the year 2012 with the CMS detector at the LHC. The observed number of events are consistent with the SM background contributions estimated from the data. The results are presented in the context of simplified models, where final states are described by the pair production of new particles decaying either to one or two jets and a weakly interacting stable neutral particle. Squark masses below 0.75 TeV and gluino masses of up to 1.1 TeV are excluded within the studied models for $\tilde{\chi}^0$

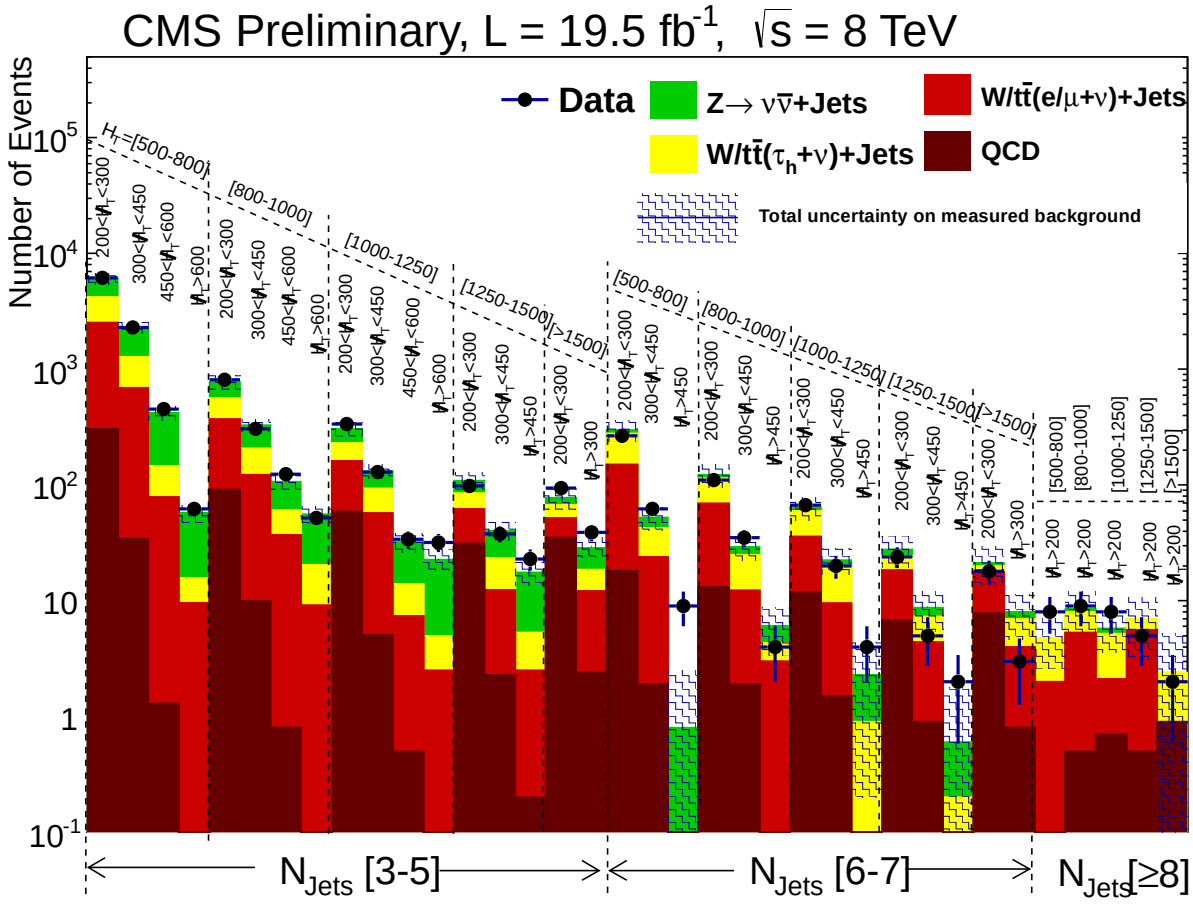

Figure 5: Summary of number of events observed in data in the 36 search regions compared to the estimated background contributions.

masses below 200 GeV.

References

[1] CMS Collaboration, "Observation of a new boson at a mass of 125 GeV with the CMS experiment at the LHC", *Phys. Lett.* **B716** (2012) 30, doi:10.1016/j.physletb.2012.08.021, arXiv:1207.7235.

[2] ATLAS Collaboration, "Observation of a new particle in the search for the Standard Model Higgs boson with the ATLAS detector at the LHC", *Phys. Lett.* **B716** (2012) 1, doi:10.1016/j.physletb.2012.08.020, arXiv:1207.7214.

[3] J. L. Feng, "Dark Matter Candidates from Particle Physics and Methods of Detection", *Ann. Rev. Astron. Astrophys.* **48** (2010) 495, doi:10.1146/annurev-astro-082708-101659, arXiv:1003.0904.

[4] J. Wess and B. Zumino, "Supergauge transformations in four dimensions", *Nucl. Phys.* **B70** (1974) 39, doi:10.1016/0550-3213(74)90355-1.

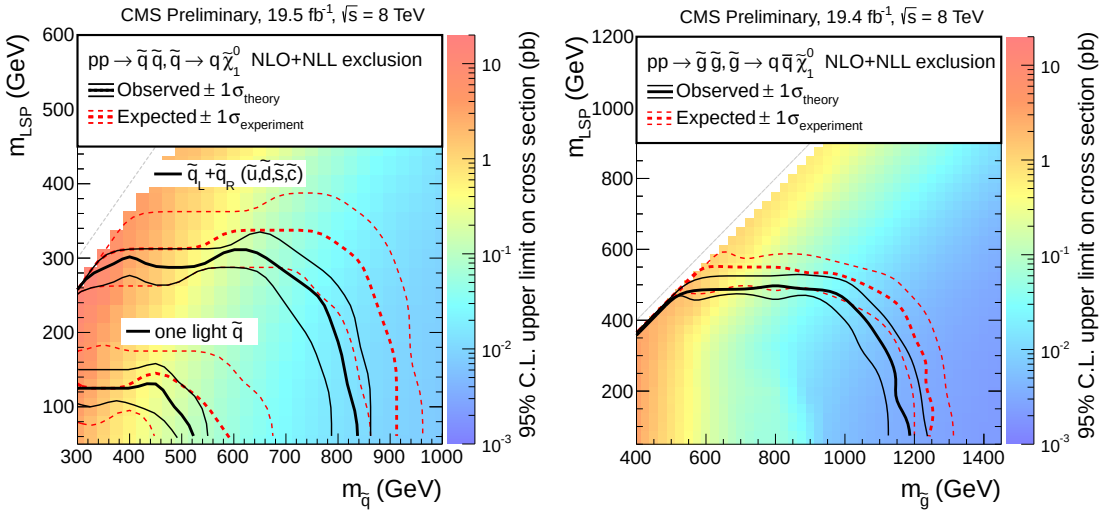

(a) Squark pair production (T2qq)

(b) Gluino pair production (T1qqqq)

Figure 6: The observed and expected 95% C.L. upper limits on the (a) $\tilde{q}\tilde{q}$ and (b) $\tilde{g}\tilde{g}$ production cross-sections in the $m_{\tilde{q}}$-$m_{\tilde{\chi}^0}$ and $m_{\tilde{g}}$-$m_{\tilde{\chi}^0}$ planes obtained with the simplified models. For the $\tilde{q}\tilde{q}$ production the upper set of curves corresponds to the scenario when the first two generations of squarks are degenerate and light, while the lower set corresponds to only one light accessible squark.

[5] H.-C. Cheng and I. Low, "TeV symmetry and the little hierarchy problem", *JHEP* **0309** (2003) 051, doi:doi:10.1088/1126-6708/2003/09/051, arXiv:hep-ph/0308199.

[6] T. Appelquist, H.-C. Cheng, and B. A. Dobrescu, "Bounds on universal extra dimensions", *Phys. Rev.* **D 64** (2001) 035002, doi:10.1103/PhysRevD.64.035002, arXiv:hep-ph/0012100.

[7] G. R. Farrar and P. Fayet, "Phenomenology of the production, decay, and detection of new hadronic states associated with supersymmetry", *Phys. Lett. B* **76** (1978) 575, doi:10.1016/0370-2693(78)90858-4.

[8] CMS Collaboration, "Search for Supersymmetry in pp Collisions at 7 TeV in Events with Jets and Missing Transverse Energy", *Phys. Lett.* **B 698** (2011) 196, doi:10.1016/j.physletb.2011.03.021, arXiv:1101.1628.

[9] CMS Collaboration, "Search for New Physics with Jets and Missing Transverse Momentum in pp collisions at $\sqrt{s} = 7$ TeV", *JHEP* **08** (2011) 155, doi:10.1007/JHEP08(2011)155, arXiv:1106.4503.

[10] CMS Collaboration, "Inclusive search for squarks and gluinos in pp collisions at $\sqrt{s} = 7$ TeV", *Phys. Rev.* **D 85** (2012) 012004, doi:10.1103/PhysRevD.85.012004, arXiv:1107.1279.

[11] CMS Collaboration, "Search for Supersymmetry at the LHC in Events with Jets and Missing Transverse Energy", *Phys. Rev. Lett.* **107** (2011) 221804, doi:10.1103/PhysRevLett.107.221804, arXiv:1109.2352.

[12] CMS Collaboration, "Search for Supersymmetry at the LHC in Events with Jets and Missing Transverse Energy", *Phys. Rev. Lett.* **109** (2012) 171803, doi:10.1103/PhysRevLett.109.171803, arXiv:1207.1898.

[13] CMS Collaboration, "Inclusive search for supersymmetry using the razor variables in pp collisions at $\sqrt{s} = 7$ TeV", *CMS-SUS-11-024* (2012) arXiv:1212.6961.

[14] CMS Collaboration, "Search for supersymmetry in hadronic final states using M_{T2} in pp collisions at $\sqrt{s} = 7$ TeV", *JHEP* **10** (2012) 018, doi:10.1007/JHEP10(2012)018, arXiv:1207.1798.

[15] CMS Collaboration, "Search for supersymmetry in final states with missing transverse energy and 0, 1, 2, or $\geq$3 b-quark jets in 7 TeV pp collisions using the variable α_{T}", *JHEP* **01** (2013) 077, doi:10.1007/JHEP01(2013)077, arXiv:1210.8115.

[16] CMS Collaboration, "Search for supersymmetry in events with b-quark jets and missing transverse energy in pp collisions at 7 TeV", *Phys.Rev.* **D 86** (2012) 072010, doi:10.1103/PhysRevD.86.072010, arXiv:1208.4859.

[17] CMS Collaboration, "Search for supersymmetry in final states with missing transverse energy and 0, 1, 2, or $\geq$3 b-quark jets in 8 TeV pp collisions", *CMS-SUS-12-028* (2013) arXiv:1303.2985.

[18] CMS Collaboration, "Search for gluino mediated bottom- and top-squark production in multijet final states in pp collisions at 8 TeV", *CMS-SUS-12-024* (2013) arXiv:1305.2390.

[19] ATLAS Collaboration, "Search for squarks and gluinos with the ATLAS detector in final states with jets and missing transverse momentum using 4.7 fb^{-1} of $\sqrt{s} = 7$ TeV proton-proton collision data", *Phys. Rev.* **D 87** (2013) 012008, doi:10.1103/PhysRevD.87.012008, arXiv:1208.0949.

[20] ATLAS Collaboration, "Hunt for new phenomena using large jet multiplicities and missing transverse momentum with ATLAS in 4.7 fb^{-1} of $\sqrt{s} = 7$ proton-proton collisions", *JHEP* **07** (2012) 167, doi:10.1007/JHEP07(2012)167, arXiv:1206.1760.

[21] A. H. Chamseddine, R. L. Arnowitt, and P. Nath, "Locally Supersymmetric Grand Unification", *Phys. Rev. Lett.* **49** (1982) 970, doi:10.1103/PhysRevLett.49.970.

[22] R. L. Arnowitt and P. Nath, "SUSY Mass Spectrum in SU(5) Supergravity Grand Unification", *Phys. Rev. Lett.* **69** (1992) 725, doi:10.1103/PhysRevLett.69.725.

[23] G. L. Kane et al., "Study of constrained minimal supersymmetry", *Phys. Rev.* **D 49** (1994) 6173, doi:10.1103/PhysRevD.49.6173, arXiv:hep-ph/9312272.

[24] J. Alwall, P. Schuster, and N. Toro, "Simplified Models for a First Characterization of New Physics at the LHC", *Phys. Rev.* **D 79** (2009) 075020, doi:10.1103/PhysRevD.79.075020, arXiv:0810.3921.

[25] CMS Collaboration, "Interpretation of searches for supersymmetry with simplified models", *CMS-SUS-11-016* (2013) arXiv:1301.2175.

[26] CMS Collaboration, "The CMS experiment at the CERN LHC", *JINST* **0803** (2008) S08004, doi:10.1088/1748-0221/3/08/S08004.

[27] CMS Collaboration, "Particle Flow Event Reconstruction in CMS and Performance for Jets, Taus and MET", CMS Physics Analysis Summary CMS-PAS-PFT-09-001, (2009).

[28] M. Cacciari, G. P. Salam, and G. Soyez, "The anti-k_t jet clustering algorithm", *JHEP* **0804:063** (2008) doi:10.1088/1126-6708/2008/04/063, arXiv:0802.1189.

[29] CMS Collaboration, "Determination of Jet Energy Calibration and Transverse Momentum Resolution in CMS", *JINST* **6** (2011) P11002, doi:10.1088/1748-0221/6/11/P11002, arXiv:1107.4277.

[30] CMS Collaboration, "Performance of Missing Transverse Momentum Reconstruction Algorithms in Proton-Proton Collisions at $\sqrt{s} = 8$ TeV with the CMS Detector", CMS Physics Analysis Summary CMS-PAS-JME-12-002, (2013).

[31] M. Cacciari and G. P. Salam, "Pileup subtraction using jet areas", *Phys. Lett.* **B 659** (2007) 119, doi:10.1016/j.physletb.2007.09.077, arXiv:0707.1378.

[32] M. Cacciari, G. P. Salam, and G. Soyez, "The Catchment Area of Jets", *JHEP* **04** (2007) 005, doi:10.1088/1126-6708/2008/04/005, arXiv:0802.1188.

[33] CMS Collaboration, "Missing transverse energy performance of the CMS detector", *JINST* **6** (2011) P09001, doi:10.1088/1748-0221/6/09/P09001, arXiv:1106.5048.

[34] J. Alwall et al., "MadGraph/MadEvent v4: The New Web Generation", *JHEP* **09** (2007) 028, doi:10.1088/1126-6708/2007/09/028, arXiv:0706.2334.

[35] T. Sjöstrand, S. Mrenna, and P. Z. Skands, "PYTHIA 6.4 Physics and Manual", *JHEP* **05** (2006) 026, doi:10.1088/1126-6708/2006/05/026, arXiv:hep-ph/0603175.

[36] N. Kidonakis, "Next-to-next-to-leading Soft-Gluon Corrections for the Top Quark Cross Section and Transverse Momentum Distribution", *Phys. Rev.* **D 82** (2010) 114030, doi:10.1103/PhysRevD.82.114030, arXiv:1009.4935.

[37] K. Melnikov and F. Petriello, "Electroweak Gauge Boson Production at Hadron Colliders through $O(\alpha(s)^2)$", *Phys. Rev.* **D 74** (2006) 114017, doi:10.1103/PhysRevD.74.114017, arXiv:hep-ph/0609070.

[38] J. Pumplin et al., "New Generation of Parton Distributions with Uncertainties from Global QCD Analysis", *JHEP* **07** (2002) 012, doi:10.1088/1126-6708/2002/07/012, arXiv:hep-ph/0201195.

[39] R. Field, "Early LHC Underlying Event Data - Findings and Surprises", arXiv:1010.3558.

[40] J. Allison et al., "Geant4 developments and applications", *IEEE 53* **1** (2006) 270, doi:10.1109/TNS.2006.869826.

[41] Z. Bern et al., "Driving missing data at next-to-leading order", *Phys. Rev.* **D 84** (2011) 114002, doi:10.1103/PhysRevD.84.114002, arXiv:1106.1423.

[42] J. H. Kuhn et al., "Electroweak corrections to hadronic photon production at large transverse momenta", *JHEP* **0603** (2006) 059, doi:10.1088/1126-6708/2006/03/059, arXiv:hep-ph/0508253.

[43] S. Ask et al., "Using γ+jets production to calibrate the Standard Model $Z(\to \nu\bar{\nu})$+jets background to new physics processes at the LHC", *JHEP* **1110** (2011) 058, doi:10.1007/JHEP10(2011)058, arXiv:1107.2803.

[44] Z. Bern et al., "Missing Energy and Jets for Supersymmetry Searches", *Phys. Rev. D* **87** (2012) 034026, doi:10.1103/PhysRevD.87.034026, arXiv:1206.6064.

[45] CMS Collaboration, "Measurement of the inclusive W and Z production cross sections in pp collisions at $\sqrt{s} = 7$ TeV with the CMS experiment", *JHEP* **10** (2011) 132, doi:10.1007/JHEP10(2011)132, arXiv:1107.4789.

[46] M. Botje et al., "The PDF4LHC Working Group Interim Recommendations", arXiv:1101.0538.

[47] K. Nakamura and others (Particle Data Group), "PDG", *JPG* **37** *075 021* (2010). http://pdg.lbl.gov.

[48] B. Efron, "The Jackknife, The Bootstrap and Other Resampling Plans", volume 38 of *CBMS-NSF Regional Conference Series in Applied Mathematics*. SIAM, Philadelphia, 1982.

[49] W. Beenakker, R. Höpker, M. Spira, and P. M. Zerwas, "Squark and gluino production at hadron colliders", *Nucl. Phys.* **B 492** (1997) 51, doi:10.1016/S0550-3213(97)00084-9.

[50] A. Kulesza and L. Motyka, "Threshold resummation for squark-antisquark and gluino-pair production at the LHC", *Phys. Rev. Lett.* **102** (2009) 111802, doi:10.1103/PhysRevLett.102.111802.

[51] A. Kulesza and L. Motyka, "Soft gluon resummation for the production of gluino-gluino and squark-antisquark pairs at the LHC", *Phys. Rev.* **D 80** (2009) 095004, doi:10.1103/PhysRevD.80.095004.

[52] W. Beenakker et al., "Soft-gluon resummation for squark and gluino hadroproduction", *J. High Energy Phys.* **12** (2009) 041, doi:10.1088/1126-6708/2009/12/041.

[53] W. Beenakker et al., "Squark and gluino hadroproduction", *Int. J. Mod. Phys.* **A 26** (2011) 2637, doi:10.1142/S0217751X11053560.

[54] M. Kramer et. al., "Supersymmetry production cross sections in ppcollisions at $\sqrt{s} = 7$ TeV", arXiv:1206.2892.

[55] A. L. Read, "Presentation of search results: the CLs technique", *Journal of Physics G: Nucl. Part. Phys.* **28** (2002) 2693, doi:10.1088/0954-3899/28/10/313.

[56] T. Junk, "Confidence level computation for combining searches with small statistics", *Nuclear Instruments and Methods* **A434** (1999) 435, doi:10.1016/S0168-9002(99)00498-2, arXiv:hep-ex/9902006.

[57] ATLAS and CMS Collaborations, "Procedure for the LHC Higgs boson search combination in Summer 2011", ATL-PHYS-PUB-2011-011, CMS NOTE-2011/005, (2011).

[58] P. M. Nadolsky et al., "Implications of CTEQ global analysis for collider observables", *Phys. Rev.* **D 78** (2008) 013004, doi:10.1103/PhysRevD.78.013004, arXiv:0802.0007.

[59] A. Martin et al., "Parton distributions for the LHC", *Eur. Phys. J.* **C 63** (2009) 189, doi:10.1140/epjc/s10052-009-1072-5, arXiv:0901.0002.